The Conformation of the Isoprenyl Chain Relative to the Semiquinone Head in the Primary Electron Acceptor (Q_A) of Higher Plant PSII (Plastosemiquinone) Differs from that in Bacterial Reaction Centers (Ubisemiquinone or Menasemiquinone) by ca. 90°[†,‡]

Ming Zheng and G. Charles Dismukes*

Department of Chemistry, Princeton University, Princeton, New Jersey 08544

Received September 18, 1995; Revised Manuscript Received April 17, 1996[⊗]

ABSTRACT: The conformation and partial electron spin density distribution of the reduced primary electron acceptor (Q_A^-), a plastosemiquinone-9 (PQ-9^-) anion radical, in photosystem II protein complexes from spinach as well as free PQ-9^- in solution have been determined by EPR and ^{1}H ENDOR spectroscopies. The data show that the conformation of the isoprenyl chain at Cβ relative to the aromatic ring differs by 90° for Q_A^- in higher plant PSII versus both types of bacterial reaction centers, *Rhodobacter sphaeroides* and *Rhodopseudomonas viridis* [containing ubiquinone (UQ) or menaquinone (MQ) at Q_A site, respectively]. This conformational distinction between the Q_A^- species in PSII vs bacterial RCs follows precisely the conformational preferences of the isolated semiquinone anion radicals free in solution; type II semiquinones like PQ-9^- have the isoprenyl CβCγ bond coplanar with the aromatic ring, while type I semiquinones like UQ^- and MQ^- place the CβCγ bond perpendicular to the ring. This conformational difference originates from nonbonded repulsions between the isoprenyl chain and the C6 methyl group present in type I semiquinones, forcing the perpendicular conformation, but absent in type II semiquinones having the smaller H atom at C6. Thus, the Q_A binding site in both higher plant PSII and bacterial reaction centers accommodates the lower energy conformation of their native semiquinones observed in solution. The energy difference between ground (CβCγ bond perpendicular to the ring) and excited (CβCγ bond coplanar with the ring) conformations of UQ^- and vitamin K_1^- radicals is estimated to be sufficiently large (ca. 6 kcal/mol) to produce greater than a 10-fold difference in populations of these conformations at room temperature. For PQ-9^-, a similar number is estimated. We propose that the strong conformational preferences of type I and type II semiquinones has lead to the evolution of different reaction center protein structures surrounding the isoprenyl/quinone head junction of Q_A to accommodate the favored low energy conformers. This predicted difference in protein structures could explain the low effectiveness (high selectivities) observed in quinone replacement experiments for type II vs type I quinones seen in higher plant PSII and bacterial reaction centers, respectively.

A pair of quinone molecules bridged by a non-heme iron−protein complex $Fe^{2+}(His)_4$, comprising part of the electron transfer chain, can be found in the reaction centers of many photosynthetic organisms. The primary quinone, or Q_A,[1] is tightly bound to the protein; its hydrophobic microenvironment ensures that it can accept only one electron. Q_A functions to shuffle electrons one at a time from the photoexcited special chlorophyll pair, via pheophytin, to the secondary quinone Q_B. Upon receiving two electrons from Q_A and picking up two protons from the medium, Q_B is reduced to its hydroquinone form which binds more weakly to the protein and is subsequently replaced by an oxidized quinone molecule from the membrane-bound quinone pool.

The atomic level three-dimensional structure of the iron−quinone complex is known from the crystal structures of two types of bacterial reaction center proteins from non-oxygenic bacteria (Figure 1) (Deisenhofer et al., 1985), but the corresponding part in the oxygenic photosynthetic organisms is not known. However, many physicochemical studies have indicated that the iron−quinone complex in oxygenic PSII reaction centers is similar in many respects to its counterpart in the bacterial reaction center (Michel & Deisenhofer, 1988; Mattoo et al., 1989; Diner et al., 1991). How far this similarity can be carried is unclear. It is known that the bidentate Glu ligand to Fe found in bacterial reaction centers (Figure 1) is absent in the analogous sequence region of higher plants, which bind instead a bicarbonate ligand (Diner & Petrouleas, 1990; Petrouleas & Diner, 1990; Xu et al., 1991). Another important distinction is the chemical structure of the native quinone molecule itself. In non-oxygenic photosynthetic reaction centers, the quinone can be either menaquinone (MQ) or ubiquinone (UQ), whereas in PSII only plastoquinone-9 (PQ-9) is found at the Q_A site *in vivo* (see Figure 2 for structures). Most biological quinones including these possess a carbon chain 45−50 atoms long (isoprenyl tail) attached to the ring at C5. The orientation

[†] Supported by NIH Grant GM39932. M.Z. acknowledges molecular biophysics Training Grant GM08309. A NATO travel grant (870733) is also acknowledged.

[‡] Preliminary results were presented at the Xth International Congress on Photosynthesis, Montpellier, France, August 1995 (Zheng et al., 1995).

[⊗] Abstract published in *Advance ACS Abstracts,* June 15, 1996.

[1] Abbreviations: ENDOR, electron nuclear double-resonance spectroscopy; EPR, electron paramagnetic resonance spectroscopy; PQ-9, plastoquinone-9; PSII, photosystem II; Q_A, the first quinone acceptor of photosystem II.

S0006-2960(95)02220-3 CCC: $12.00

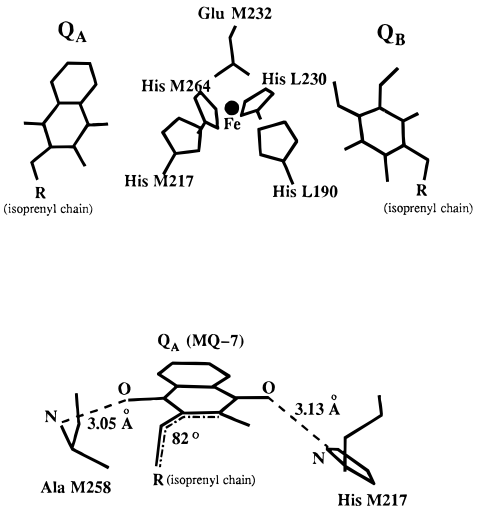

FIGURE 1: Structure of the Iron-quinone complex in *Rps. viridis* reaction center from the Brookhaven PDB entry 1prc. Upper panel: $Q_A-Fe^{2+}-Q_B$ complex and ligands that bind to Fe^{2+}. Lower panel: hydrogen bonding environment of Q_A.

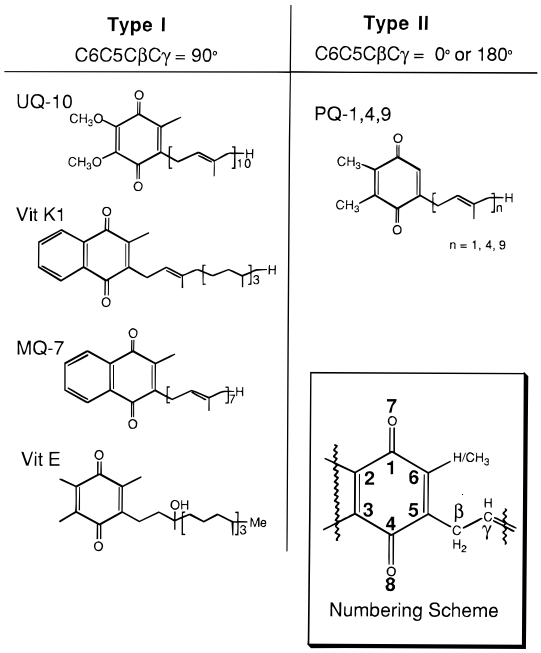

FIGURE 2: Structure of various quinones that are discussed in the text. The numbering scheme used in the text is also shown. The classification is based on the hyperfine coupling constants of β-methylene protons and their derived conformation. Hyperfine data for type I quinones are from Das et al. (1970), whereas those for type II quinones are from Pederson (1978, 1985) and this work.

which the tail makes with the quinone head is not random but depends on the substitution pattern on the ring. Type I (bacterial) quinones have a methyl group at C6, whereas type II (higher plant) quinones have a hydrogen atom at C6 (Figure 2). An unexplained observation is why these two classes of quinones are not capable of functionally replacing one another in electron transport at comparable concentrations (Krogmann et al., 1962; Trebst et al., 1963; Klimov et al., 1980). Do these quinones interact differently with the reaction center environments of their respective proteins?

We offer answers to some of these questions in this work by investigating the structure of the plastosemiquinone anion radical both free in solution and bound to the Q_A site of PSII in spinach, using electron nuclear double resonance (ENDOR) spectroscopy. A prerequisite for ENDOR study of Q_A^- is to eliminate the magnetic influence of the paramagnetic Fe^{2+}. In the present work, the cyanide treatment method is used which relies on binding of the strong-field ligand cyanide to Fe^{2+}, thereby converting it from its high spin ($S = 2$) configuration to the low spin ($S = 0$) state (Sanakis et al., 1994).

MATERIALS AND METHODS

PQ-9 Anion Radical. The PQ-9 anion radical ($PQ\text{-}9^-$) was generated by dissolving purified microcrystalline PQ-9 powder into degassed 2-propanol solvent containing ~5 mM KOH. The concentration of PQ-9 was ~1mM. The resulting greenish solution was loaded into EPR tubes (1 × 2 for liquid solution EPR and ENDOR samples and 3 × 4 for frozen solution EPR and ENDOR samples) which were sealed subsequently for measurements. The entire procedure was carried out in argon atmosphere. PQ-9 was a gift from Hoffman-La Roche and Company, Basel, Switzerland.

Spinach PSII Sample Preparation and Cyanide Treatment. PSII membrane particles of BBY type were prepared according to the procedure by Berthold et al. (1981), modified by Ford and Evans (1983). PSII core complexes for spinach were prepared according to the procedure by Ghanotakis et al. (1987).

Cyanide treatment basically follows the procedure given by Sanakis et al. (1994). PSII particles were first centrifuged to remove excess buffer solution and resuspended to a Chl concentration of ~0.3 mg/ml in a 0.3 M NaCN solution at pH = 8 containing 40 mL of 0.1 M Tricine buffer, followed by dark incubation at 4 °C. The amount of incubation time varied from 1 h to 3 days, the latter time being used for $^2H-$water exchange. After incubation the sample was centrifuged and resuspended in the same solution to a final concentration of ~10 mg Chl/mL. To this solution was added one-tenth volume of freshly made 0.4 M dithionite solution, followed by 5 min of dark incubation. Samples were loaded into 3 × 4 mm quartz tubes and frozen immediately. ^2H_2O exchange was carried out by using solutions made with 99.9% ^2H_2O (Cambridge Isotope Laboratories). Quantification of the radical was done by double integration of the EPR signal and typically found 0.6 spins/PSII, using tyrosine-D in an untreated control as internal standard. This yield is consistent with the previous literature result (Sanakis et al., 1994) . Interference from Tyr D^+, Tyr Z^+, and Chl^+ radicals was avoided by adding excess dithionite and doing all preparations in dim light or darkness. The ENDOR spectra of all these radicals have been independently generated and differ from that of Q_A^-.

EPR, ENDOR, and Special TRIPLE. All of the magnetic resonance measurements were carried out on a Bruker ESP 300 spectrometer equipped with the ER250 ENDOR accessory. Variable temperatures were achieved via a Bruker liquid nitrogen flow system ER4111VT. EPR spectra were recorded with a Bruker ER4102 cavity resonating in the TE_{102} mode. ENDOR and Special TRIPLE spectra were recorded with a Bruker cavity and Bruker rf helix/dewar resonating in the TM_{110} mode.

RESULTS

PQ-9− in Liquid Phase

Liquid solution EPR, ENDOR, and Special TRIPLE measurements were performed on $PQ\text{-}9^-$. Figure 3 shows

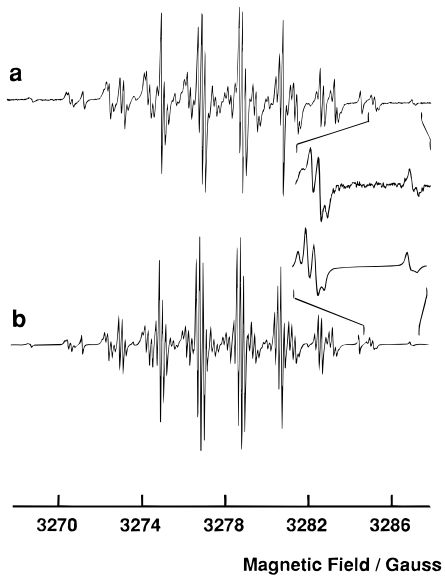

FIGURE 3: EPR spectra of PQ-9$^-$ in 2-propanol solvent. (a) Experimental spectrum. (b) Simulation using hyperfine parameters given in the top row of Table 1. EPR conditions: modulation amplitude = 0.03G, microwave frequency = 9.22 GHz, T = 290K.

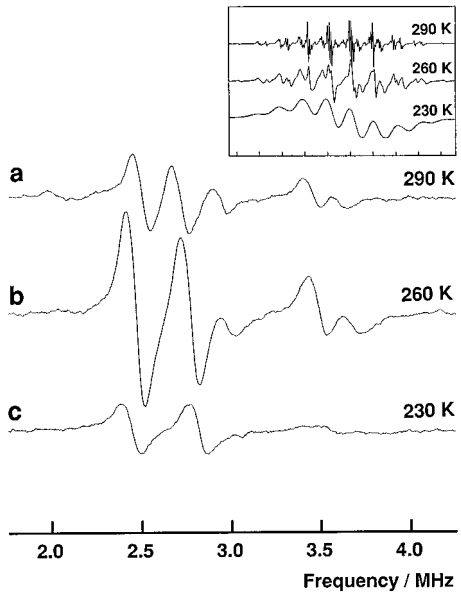

FIGURE 4: Special TRIPLE spectra of PQ-9$^-$ in 2-propanol solvent. (a) T = 290 K, (b) T = 260 K, (c) T = 230 K. Parameter settings: microwave frequency = 9.56 GHz, microwave power = 9 dB, rf power A_1 = 11dB, A_2 = 5dB, A_3 = 3 dB, rf modulation amplitude = 100 kHz.

the EPR spectrum of PQ-9$^-$ in fluid solution measured at 290K, and a simulation using hyperfine parameters obtained directly from the ENDOR and Special TRIPLE measurements. Figure 4 shows the Special TRIPLE spectra of PQ-9$^-$ measured at three different temperatures. The assignments of the hyperfine couplings, summarized in Table 1 and Figure 5, were made using several constrains: (1) quantitative agreement with the EPR simulation; (2) explanation of the strong temperature dependence of the ENDOR peaks (peaks for the ring α- and β-methylene protons are more temperature-dependent than methyl protons); and (3) agreement with the peak intensities in the Special TRIPLE spectra (which is proportional to the number of nuclei). These assignments are compared to the results of MacMillan et al. (1995) in Table 1.

As can be seen from Table 1, for the α-ring and methyl protons, our results are in good agreement with those of MacMillan et al., the difference being less than 0.22 MHz. But for the C5 isoprenyl β-H and γ-H couplings, our results differ substantially. We have tried several conditions to detect the small 0.3 MHz γ-H coupling by ENDOR without success. The absence of the γ-H coupling in our case is fully consistent with our EPR simulation which rigorously excludes the existence of a small hyperfine coupling of this magnitude. Another important difference is that we see clearly an axial hyperfine tensor for the two isoprenyl β-H's in EPR, ENDOR (not shown), and Special TRIPLE spectra of PQ-9$^-$, whereas MacMillan et al. detected a single isotropic hyperfine coupling for the two β-H's. We attribute the observed β-H hyperfine anisotropy to the slower tumbling rate of the isoprenyl chain relative to the ring α-H and methyl protons, all of which have additional degrees of rotational freedom. This interpretation is supported by the observation that decreasing the temperature increases the β-H hyperfine anisotropy, as shown in the Special TRIPLE spectra in Figure 4. The isotropic part of the isoprenyl β-H couplings observed by us is very close to that reported by MacMillan et al., the difference being less than 0.3 MHz (Table 1). The differences between our results and those of Macmillan et al. might arise from the purity of the isopropanol solvent. Our sample behaves as though the solvent is more viscous, which is why we can see a temperature-dependent anisotropic hyperfine coupling for the isoprenyl β-H's and observe no γ-H coupling at all, since it is even more anisotropic and dependent on isoprenyl chain conformation. The presence of water in the solvent or different degrees of ion-pairing between the semiquinone radical and the counter cation (K^+), which is a function of concentration, may account for the small differences in isotropic couplings. It is well documented that hyperfine couplings from semiquinones are very sensitive to solvents (Pedersen, 1985).

Q_A− in PSII

Special Triple Spectra of Q_A^-. EPR measurements were performed using cyanide-treated spinach PSII membranes and core complexes in both H_2O and ^2H_2O buffers. These data will are presented and discussed in detail in a separate paper that focuses on the interaction of Q_A^- with the PSII environment. To directly measure Q_A^- proton hyperfine couplings, we have used the Special TRIPLE spectroscopy, which yields a factor of 2 increase in sensitivity and a slight increase in spectral resolution compared to conventional ENDOR spectroscopy. For solution phase radicals, the advantage of the Special TRIPLE detection mode over the ENDOR mode in terms of sensitivity and resolution is well established (Kurreck et al., 1988). For frozen solutions, we are unaware of direct comparisons, but one can also expect similar improvements (Kurreck et al., 1984) . Figure 6 shows the Special TRIPLE spectra for the frequency region which include hyperfine couplings larger than or equal to 2 MHz, obtained from both spinach PSII membranes (a−d) and core complexes (e) at 135 K (a and b) and 200 K (c and d) and in H_2O (a and c) and ^2H_2O (b and d) buffer. As can be seen, the pair of resolved transitions labeled d−d′ and e−e′ in PSII membranes seen at 135 K merges into a single unresolved, broad peak at 200 K. This conversion was monitored at intermediate temperatures (not shown). In the PSII core complexes, the corresponding pair of transitions

Table 1. Liquid Phase ^{1}H ENDOR Assignments for PQ-9 Anion Radical (Units MHz)

2 and 3-CH_3	5 β-CH_2	6α-H	5γ-H	temp (K) and solvent	reference
4.998, 5.432	6.922 ($A_\perp$), 7.273 ($A_{||}$), 7.039 (A_{iso})	5.868	not detected	T = 290 K 2-propanol	this work
4.926, 5.544	6.982 ($A_\perp$), 7.418 ($A_{||}$), 7.127 (A_{iso})	5.960	not detected	T = 260 K 2-propanol	this work
4.943, 5.322	6.870	5.740	0.306[a]	T = 263 K 2-propanol	MacMillan et al. (1995)

[a] Detected at T = 293 K.

Table 2. ^{1}H Hyperfine Couplings of $Q_A^{\bullet-}$ in PSII Measured at 135 K

transitions	hyperfine couplings (MHz)	tentative assignment
d−d′	2.7	$-CH_2$ $A_\perp$
e−e′	3.3	$-CH_2$ $A_\perp$
f−f′	4.0	α-H $A_{||}$
g−g′	5.3	$-CH_3$ $A_\perp$
h−h′	5.7	$-CH_3$ $A_\perp$
i−i′	6.6	$-CH_3$ $A_{||}$
j−j′	7.4	$-CH_3$ $A_{||}$
k−k′	8.6	α-H $A_\perp$

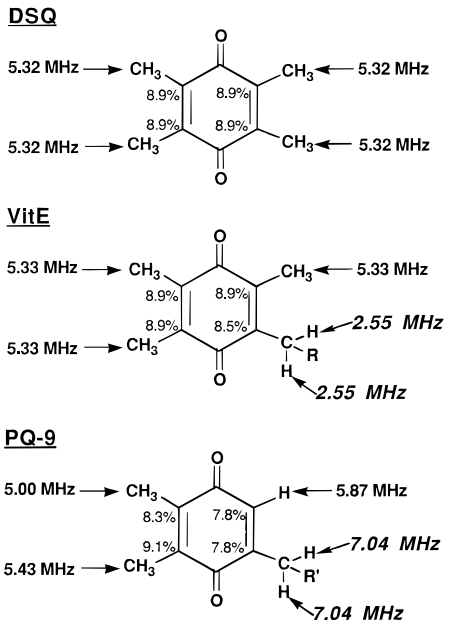

FIGURE 5: Hyperfine coupling assignment for PQ-9 and related anion radicals and the derived π electron spin densities, For easy comparison, only isotropic values for the β protons of PQ-9$^-$ are shown. Data for durosemiquinone and Vit E semiquinone anion radicals are from literature (Das et al., 1970) .

could not be resolved and appear as a single broad peak at all temperatures examined between 135 and 200 K.

^{1}H Hyperfine Assignment of Resonance Peaks Observed for Q_A^-. To extract structural information from our Special TRIPLE data, assignments of the resonance peaks shown in Figure 6 have to be made.

(a) Methyl Protons. It is a well established experimental fact that the freely rotating methyl protons in all organic radicals have an axial hyperfine tensor with anisotropy ranging from 10 to 40% with $|A_\perp| < |A_{||}|$ (Hyde et al., 1968; Kurreck et al., 1984; O'Malley & Babcock, 1984; Feher et al., 1985) . In Q_A^-, transitions g−g′, h−h′, i−i′, and j−j′ (Figure 6) are thought to arise from the two freely rotating methyl groups. Four reasons lead us to this assignment: (1) the powder pattern lineshapes exhibited by these transitions are typical of axial tensors with g−g′ and h−h′ = $A_\perp$, and e−e′ and j−j′ = $A_{||}$; (2) increasing the temperature from 135 to 200 K sharpens these transitions, which can be understood

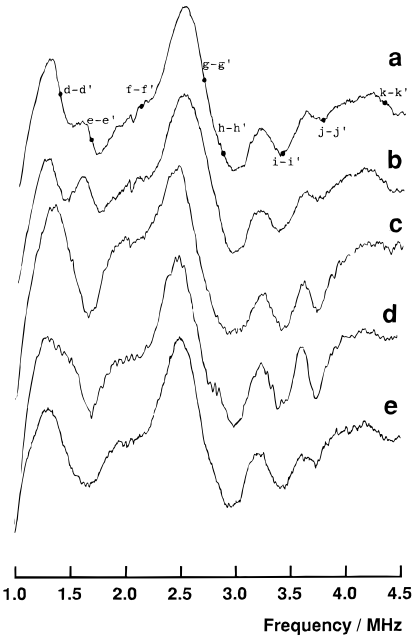

FIGURE 6: Special TRIPLE spectrum of Q_A^- from cyanide treated PSII membranes. (a) Spinach PSII membranes in H_2O buffer, T = 135K. (b) Spinach PSII membranes in ^2H_2O buffer, T = 135 K. (c) Spinach PSII membranes in H_2O buffer, T = 200 K. (d) Spinach PSII membranes in ^2H_2O buffer, T = 200 K. (e) Spinach core complex in H_2O buffer, T = 135 K. Parameter settings: microwave frequency = 9.55 GHz, microwave power = 22 dB (19 dB when at 200 K), rf power A_1 = 11dB, A_2 = 5dB, A_3 = 0 dB, rf modulation amplitude = 100 kHz, rf central frequency = 14.50 MHz, sweep time = 5.12 s, number of scans = 2400.

as due to faster methyl rotation at higher temperature and thus more complete motional narrowing; (3) these peaks are the most intense ones in the spectrum and thus should come from the most abundant protons; (4) although we do not know how to choose pairs of transitions into two axial hyperfine tensors, the upper and lower bound to the isotropic coupling constant can be calculated and compared to the measured isotropic coupling of free PQ-9$^-$ anion radical. These are 6.26 (= $[2A_{h-h'} + A_{j-j'}]/3$) and 5.71 (= $[2A_{g-g'} + A_{i-i'}]/3$) MHz. These values can be compared with the observed isotropic coupling for the methyl groups in the PQ-9 anion radical in 2-propanol at 260−290 K (5−5.5 MHz, Table 1).

(b) Ring α Proton. In general, due to the short distance between an α proton and the spin density, a high degree of anisotropy is expected for the hyperfine tensor (Kevan & Kispert, 1976) . This causes a broad and weak ENDOR intensity distribution for α protons and makes them difficult to detect. For the *p*-benzosemiquinone anion radical, both theoretical prediction (O'Malley & Babcock, 1986) and experimental measurement (Hales, 1975; O'Malley & Babcock, 1986; Burghaus et al., 1993) indicate that α protons have an approximately axial hyperfine tensor with large anisotropy. For instance, Burghaus et al. have determined the hyperfine tensor for the α-H in the *p*-benzosemiquinone

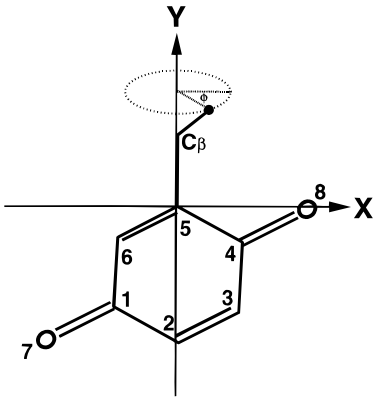

FIGURE 7: Geometry and definition used for the β proton hyperfine tensor calculation (see the text for details). Bond length (unit Å): C1C2 = 1.51, C2C3 = 1.37, C3C4 = 1.52, C4C5 = 1.51, C5C6 = 1.35, C6C1 = 1.49, C1O7 = 1.23, C4O8 = 1.23, C5Cβ = 1.52, CβHβ = 1.12. These data are obtained from an optimized PQ-9 structure using Biosym's *Builder* module. The angle ϕ corresponds to C4C5CβHβ dihedral angle. The spin densities used in the calculation are: ρ1 = 10%, ρ2 = 8.3%, ρ3 = 9.1%, ρ4 = 10%, ρ5 = 7.8%, ρ6 = 7.8%, ρ7 = 24%, ρ8 = 23%.

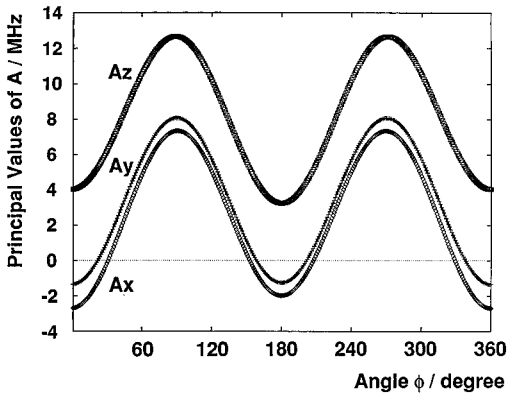

FIGURE 8: Calculated three principal values of the β proton's hyperfine tensor as a function of the dihedral angle ϕ defined in Figure 7. The calculation adopts a simple multiple point-dipole model using the partial spin densities of the PQ-9$^-$ radical measured in solution (at C2, C3, C5, C6) and those assumed from the benzosemiquinone anion radical (at C1, C4, O7, O8) as defined in the legend to Figure 7. The resulting hyperfine tensor values should be considered as only approximate as the assumption of point spin densities for π-type radicals is an especially crude approximation, in addition to the limitations of the metrical parameters of the structure and choice of spin distribution which varies with environment. The key result is the prediction of a nearly axial hyperfine tensor for β-methylene protons, in agreement with the spectral assignments for both frozen and solution forms of PQ-9$^-$.

anion radical to be −10.5, −8.7, −0.9 MHz by high frequency EPR (Burghaus et al., 1993). Since the spin density distribution in Q_A^- should approximate that of *p*-benzoquinone anion radical to first order, a similar range of hyperfine anisotropy for the α proton in Q_A^- is expected. We therefore tentatively assign transitions f−f′(4.00 MHz) and k−k′(8.60 MHz) (Figure 6) to be the parallel and perpendicular hyperfine components of the α proton based on their positions and weak intensities. The d−d′ and e−e′ transitions may be excluded because they are relatively strong and temperature-dependent.

(c) β-Methylene Isoprenyl Protons. Kevan and Kispert (1976) have compiled 10 cases of hyperfine tensors of β-methylene protons in organic radicals with localized π spin density. In all cases cited, a nearly axial hyperfine tensor with $A_{\|} > A_{\perp} > 0$ is found. Since the anisotropic hyperfine interaction can be well estimated using the point-dipole model when a proton is two bonds away from the π spin density (O'Malley & Babcock, 1986), an axial tensor for a β-methylene proton is expected. Hyperfine data for the β-methylene protons in aromatic radicals are rare, especially benzosemiquinones with delocalized π spin density. To establish a spectral assignment, we have calculated the hyperfine tensor of the β-methylene proton in the benzoquinone anion radical using the multipoint-dipole model (Figure 7). The bond length and spin density distribution used in the calculation are given in the legend to Figure 7. The atomic π spin densities in Figure 7 were reduced to single points centered at each atom. Figure 8 shows the calculated three principal values of the β-methylene hyperfine tensor as a function of its orientation. While the magnitude of the principal values does not accurately agree with experiment—varying with the choice of spin density distribution, bond lengths and especially the crude approximation of point spin densities—the nearly axial symmetry of the hyperfine tensor is predicted. This result is consistent with the β-methylene isoprenyl hyperfine couplings we have measured for PQ-9$^-$ in the liquid phase (Table 1) and in frozen solution. Since an average of the axial hyperfine tensor of a β-methylene proton over all of its possible orientations still yields an axial tensor, this simple point-dipole model predicts an axial hyperfine tensor for methyl protons too. This latter result of the point-dipole model is again consistent with the experimental observation that methyl protons in semiquinone anion radicals usually have axial hyperfine tensors.

In the special TRIPLE spectra of Q_A^- in Figure 6, transitions d−d′ (2.7 MHz) and e−e′ (3.3 MHz) have the same strong temperature dependence from 135 to 200 K, collapsing to form a single peak at the higher temperature. The same two peaks are also replaced by a single peak in core complexes at the same position as observed in PSII membranes even at the lower temperature (Figure 6d). This behavior indicates that the d−d′ and e−e′ transitions are sensitive not only to temperature but also to the extent of detergent extraction used to separate PSII centers from the thylakoid membrane. On the basis of these observations, we assign the d−d′ and e−e′ transitions to the perpendicular hyperfine tensor component of two different β-methylene protons of the isoprenoid chain. The parallel components are expected to be at much higher frequency and thus too weak to detection. With this assignment, the experimental behavior of these transitions can be readily explained. At 135 K and below, a static conformation of Q_A^- is trapped, which results in resolved transitions from the two β-methylene isoprenyl protons. At 200 K, an increased torsional oscillation averages out the difference between the two β protons, causing them to merge at an intermediate frequency. In core complexes, both the Q_A and Q_B acceptor sites are known to be disrupted relative to PSII membranes, resulting in altered affinities and a wider range of physicochemical properties (Ghanotakis & Yocum, 1986; Ghanotakis et al., 1987). Consequently, a lower potential barrier for the quinone head−tail torsional oscillation should be expected, resulting in faster torsional oscillation even at 135 K and thus a single merged transition.

We have also considered the possibility that the d−d′ and e−e′ transitions might belong to two components (A_x, A_y)

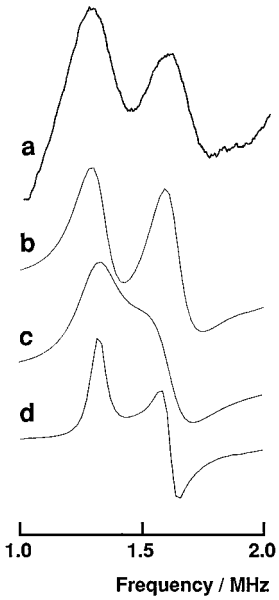

FIGURE 9: Line shape comparison for the d−d′ and e−e′ Special TRIPLE transitions from Figure 6. (a) Experimental spectrum obtained from a cyanide-treated BBY (in ^2H_2O buffer) sample at 135 K. (b) Simulation using two axial hyperfine tensors: (A_x, A_y, A_z) = (2.7, 2.7, 15) and (3.3, 3.3, 15) MHz, and a line width of 100 KHz. (c and d) Simulations using one rhombic tensor (A_x, A_y, A_z) = (2.7, 3.3, 15) MHz, with a line width of 100 kHz in curve c and 30 kHz in curve d, respectively.

of a single β-methylene proton hyperfine tensor. Figure 9 shows the line shape comparison between the experimental spectrum and the simulated spectra using two different assumptions; only part of each spectrum is shown here for the sake of simplicity. Curve b is obtained by using two different axial hyperfine tensors: (A_x, A_y, A_z) = (2.7, 2.7, 15) and (3.3, 3.3, 15) MHz, and a line width of 100 kHz. Curves c and d are obtained by using one rhombic tensor (A_x, A_y, A_z) = (2.7, 3.3, 15) MHz, with a line width of 100 kHz in curve c and 30 kHz in curve d, respectively. It is very clear that the experimental spectrum resembles curve b, corresponding to two distinct β-methylene protons. Moreover, using the methyl proton transitions g−g′ and h−h′ as a internal intensity standard, we can see that the combined d−d′ and e−e′ transition intensity is too strong to be attributed to a single β-methylene proton, assuming equal ENDOR enhancements (Figure 6d).

DISCUSSION

Solution Conformation of PQ-9−

Spin Density Distribution of PQ-9⁻. The measured hyperfine couplings shown in Figure 5 can be used to derive the spin density distribution of the unpaired π electron and the conformation of the β-methylene protons by using well-established empirical formulae. For α-protons there is the McConnell relationship (McConnell & Chesnut, 1958):

$$a_{\alpha-H}{}^{H} = Q_{CH}{}^{H}\rho_C{}^{\pi} \qquad (1)$$

where $Q_{CH}{}^{H}$ is a constant having the value −75 MHz for 1,4-benzosemiquinones (Das et al., 1970), and $\rho_C{}^{\pi}$ is the spin density at the α carbon. For β-methylene or methyl protons, the Mclachlan formula is used (McLachlan, 1958; Heller & McConnell, 1960; Lykos, 1960):

$$a_{\beta-H}{}^{H} = (B_0 + B_1 \cos^2\theta)\rho_C{}^{\pi} \qquad (2)$$

where B_0 is a constant that is close to zero, and B_1 is also a constant with a value of 120 MHz typically adopted for 1,4-benzosemiquinones (Das et al., 1970). For freely rotating methyl protons, eq 2 can be simplified to eq 2′:

$$a_{ME}{}^{H} = (B_1/2)\rho_C{}^{\pi} \qquad (2')$$

Using these equations, we have converted the hyperfine couplings into the spin density distribution within the aromatic ring, as shown in Figure 5. For comparison, data for durosemiquinone (DSQ) and vitamin E semiquinone are also shown in Figure 5 (Das et al., 1970). The spin densities we find for the PQ-9 anion radical are consistent with those obtained by others on various 2,3,5,6-alkyl-substituted-1,4-benzosemiquinones in solution (Das et al., 1970; Sullivan et al., 1970). It has been found that, for various alkyl substitution at the ring positions, the spin densities at these positions do not change very much in solution phase, being in the range of 7∼9% (Das et al., 1970; Sullivan et al., 1970).

Stereochemistry of the PQ-9 Anion Radical in Solution. The derivation of the spin density at C5, where the isoprenyl chain connects, is worth reviewing. The hyperfine couplings for the two β-methylene isoprenyl protons connected to Cβ are equivalent and the largest among all the protons at 7.04 MHz. In Figure 5, we have compared the isotropic hyperfine couplings obtained for selected semiquinones in liquid phase. As can be seen, the β-methylene isoprenyl proton couplings in PQ-9⁻ are 2.76 times higher than those in vitamin E. In the case of semiquinone anion radicals of vitamin E, vitamin K1, ubiquinone-10, and other related species, it was found that the hyperfine couplings for the β-methylene protons of the side chain (2∼3 MHz) are about half of that for the ring methyl protons (5∼6MHz) (Das et al., 1970). The greatly reduced β-methylene proton coupling in all these cases provides clear evidence that θ in eq 2, the dihedral angle between the axis of the C5 p_z orbital, and the direction of the Cβ-H bond, is equal to ∼60° for both β-methylene protons in the lowest energy conformation. This stereochemistry can also be represented by a ∼90° dihedral angle of C6C5CβCγ for the isoprenyl chain relative to the ring (Figure 10a). In the case of the PQ-9⁻, it is also necessary to have equivalent dihedral angles for the two β-protons in order to explain their equivalent coupling constants. This can only be realized by choosing θ to be either 60° or 30°. The first choice yields a spin density of 22.6% at C5. This high spin density cannot be rationalized without assuming a drastic effect of the isoprenoid chain on the spin density distribution within the aromatic ring, which is inconsistent with the other coupling constants and has never been observed before for similar systems. On the other hand, by choosing θ to be 30° in eq 2, we obtain a spin density of 7.8% at C5, a value which is similar to that at positions 2, 3, and 6, as it should be, and, moreover, consistent with values found for semiquinones in liquid phase (Das et al., 1970). The C6C5CβCγ dihedral angle in PQ-9⁻ is thus 0° or 180°, placing the isoprenyl chain in the plane of the quinone ring (Figure 10c). This angle differs by 90° from that for all type I semiquinones, including vitamins E, K_1, and UQ-10 anion radicals (Figure 2). The C6C5CβCγ = 180° conformation is expected to be higher in energy than C6C5CβCγ = 0°, as this will cause steric repulsions between

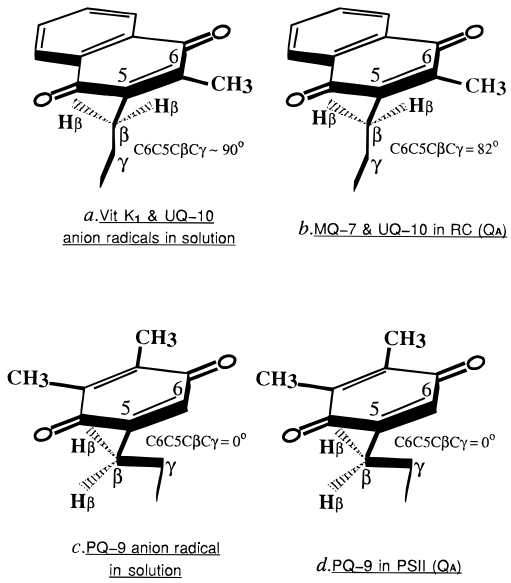

FIGURE 10: Conformation of various quinones and semiquinones. (a) Solution conformation of vitamin K1 and UQ-10 anion radicals. (b) Conformation of menaquinone in *Rps. viridis* reaction center (Q_A site). (c) Solution conformation of PQ-9 anion radical. (d) Conformation of Q_A^- ($PQ\text{-}9^-$) in PSII as derived from ENDOR data.

the carbonyl oxygen and the Cγ substituents. Thus Cγ is expected to be both in the ring plane and close to the C6 position than to the carbonyl.

For simplification of our following discussion, we have divided the quinone molecules shown in Figure 2 into two types based upon the large difference in β-methylene proton hyperfine constants and the derived solution conformation of their corresponding anion radicals [C6C5CβCγ = 90° (type I) vs 0° or 180° (type II)]. Comparison of the ring substitution patterns of these two groups reveals that the presence or absence of a methyl group at C6 is responsible for the conformational difference between the anion radicals in the two classes.

Conformation of Q_A^-: PSII vs. bacterial RC's

Conformation of Q_A^-. As we have mentioned in the previous section, the d−d′ and e−e′ transitions in Figure 6 have been assigned to the perpendicular components of the two β isoprenyl protons in Q_A^-. Because these transitions are very close to each other in frequency, the two β isoprenyl protons see roughly the same spin density. This argues strongly for a symmetric placement of the two β-methylene protons about the aromatic ring (Figure 10d), a conformation identical to that for $PQ\text{-}9^-$ in solution.

Our ENDOR data thus suggest that the conformation of Q_A^- in PSII resembles the solution conformation of $PQ\text{-}9^-$. What about Q_A^- in bacterial RC's? For the *Rb. sphaeroides* RC's, according to a recently obtained 2.65 Å resolution structure (Ermler et al., 1994), the C6C5CβCγ angle for UQ-10 at Q_A site is 82°, a number that is very close to what is found for the UQ-10 anion radical in solution (Figure 10). For the *Rps. viridis* RC, the C6C5CβCγ angle for MQ-7 at the Q_A site is also 82°. This conformation is again essentially the same as that of vitamin K_1 anion radical (a napthoquinone analog of MQ-7 anion radical) in solution (Figure 10). Therefore, the conformation of the PQ-9 isoprenyl chain relative to the semiquinone head in the Q_A site of higher plant PSII differs by ca. 90° versus both known types of bacterial reaction centers. *Importantly, the Q_A binding site in both higher plant PSII and bacterial reaction centers accommodates the most stable solution conformation of their native semiquinones.*

Energetics of Conformational Equilibria. Is this conformational difference between Q_A^- in higher plant PSII and bacterial reaction centers merely a coincidence, or is it a result of nature's attempt to achieve high quinone binding affinity at the Q_A site? To answer the above question, one really has to know the quinone head−tail conformation energetics, a subject which lacks detailed investigation at the present. But even with limited information, one can still make interesting predictions. For UQ-10 and vitamin K_1 anion radicals, the activation barrier for the head−tail rotation is ~6 kcal/mol. This number was obtained from a study of the alternating EPR line width effects caused by the molecular jumping between two thermodynamically equivalent conformations (C6C5CβCγ ~ ±90°) of the UQ-10 and vitamin K_1 anion radicals (Das et al., 1970). It gives an upper estimate of the free energy difference between UQ-10's stable conformation (C6C5CβCγ ~90°) and the higher energy conformation (C6C5CβCγ ~0° or 180°). A 6 kcal/mol energy difference corresponds to a predicted population difference of 10^4 at room temperature. For $PQ\text{-}9^-$, we do not see an alternating line width effect. We see instead only a uniform linewidth broadening in the EPR spectra (Figure 4 inset) and α-H and β-H peak broadening in ENDOR and Special TRIPLE spectra (Figure 4) when temperature is lowered from 290 to 230 K. Temperatures above 290 K lead to rapid decay of the $PQ\text{-}9^-$ radical. A direct measure of the rotational activation energy was not possible; it might be either lower or higher than 6 kcal/mol. However, a lower limit to the population difference between PQ-9's stable type II conformation and the higher energy type I conformation is estimated to be ca.10-fold at room temperature. This is estimated as follows. With the higher energy type I conformation, the β-H coupling is expected to be 2.34 MHz. Experimentally, we observe a decrease of the β-H hyperfine coupling by 0.088 MHz when increasing the temperature from 260 to 290 K (Table 1). This decrease may be due either to the population of the higher energy conformation, or to the temperature-dependent solvation effect, or both. If the former mechanism is the sole source of hyperfine coupling change, then we need less than 10% of the higher energy conformor to produce the 0.088 MHz frequency shift.

The above discussion on conformation energetics leads to the following predictions: (1) UQ-10 and MQ-7, or any other type I quinone for that matter, should have low binding affinities at the Q_A site of PSII reaction centers, in part, because it costs energy for these type I quinones to adopt the unstable (C6C5CβCγ ~0° or 180°) conformation. We estimate their binding affinity should be at least 10-fold lower than for PQ-9, if other factors (such as head group affinity) were the same. (2) Conversely, PQ-9 or any other type II quinones should have low binding affinities at the Q_A site of the bacterial reaction centers, because they have to form the unstable (C6C5CβCγ ~90°) conformation, and its binding affinity should be at least 10-fold lower than that of the native quinone UQ-10 or MQ-7.

Replacement of Q_A^-. Binding affinities of different quinone cofactors at both Q_A and Q_B sites of the *Rb. sphaeroides* RC's have been exhaustively studied. The

influence of both head group structure (Gunner, 1991) and hydrocarbon tail structure (Warncke et al., 1994) on the binding affinities has been examined. But the effect of quinone head-tail conformation on binding affinity, an aspect we are addressing here, has not been investigated in the literature. An early study by Okamura et al showed that PQ-9 can be forced into the Q_A site of the *Rb. sphaeroides* RC's under the condition of 5−20 times higher concentration than that used for UQ-10 by using both longer incubation times and higher temperature (25 °C) (Okamura et al., 1975). A quantitative comparison of the binding affinities of the two quinones has not been made.

The Q_A binding requirements in PSII have been examined indirectly in early works also. There is a report showing that the absence of a methyl group at C6 in quinones possessing a C-5 isoprenyl tail is essential for the biological activity in chloroplasts (Krogmann et al., 1962). This conclusion was reached on the basis of the capability of exogenous quinones to restore the Hill reaction ($H_2O \rightarrow$ indophenol electron transfer) in chloroplast depleted of all PQs by heptane extraction. One striking comparison is that 2,3-dimethyl-5-phytyl benzoquinone (PQ-4) was found, like PQ-9, fully functional in restoring the Hill and photophosphorylation reactions, whereas 2,3,6-trimethyl-5-phytyl benzoquinone, with only one more methyl group at C6 and thus a type I quinone in our classification, was found completely inactive in supporting the Hill reaction (Krogmann et al., 1962). Several vitamin K derivatives and ubiquinones, both containing C-5 isoprenyl chains, were also found inactive (Krogmann et al., 1962). These results are also consistent with a report by Trebst et al. (1963) showing that small quinones lacking the C-5 isoprenyl chain do reconstitute the Hill reaction, while vitamin K3, a type I quinone, does not function. This article also confirmed that UQ-10 could not support photo-reduction of exogeneous acceptors when added back to PQ-depleted thylakoids obtained by petroleum ether extraction (Trebst et al., 1963). A lower binding affinity of type I quinones at the Q_A site of PSII was more directly inferred by Klimov et al. (1980). They showed that vitamin K1 could not restore the split doublet EPR signal due to pheophytin$^-$ $-Q_A^-$−iron in PQ-depleted PSII preparations (Klimov et al., 1980). The conclusion from all these studies is that only type II quinones work in PSII at physiological concentration. A more recent work by Diner et al. (1988) has shown that UQ-9 could be incorporated into PSII core preparations isolated from *Chlamydomonas reinhardtii* that were extracted with Triton X-100 (1%), but a 20-fold higher concentration than PQ-9 was required for 50% reactivation. The results of Krogmann et al., Trebst et al., and Klimov et al. clearly support our prediction.

It is interesting to point out that two ESEEM studies on Q_A^- have appeared recently. Astashkin et al. (1995) have measured ESEEM of Q_A^- in Zn^{2+} substituted spinach PSII membranes, and Tang et al. (1995) have made the same measurement on cyanide-treated PSII core complexes from Synechocystis PCC6803. Both groups obtained similar sets of data and concluded that there are two nitrogens magnetically coupled to Q_A^-, and that one of them is from a peptide nitrogen, possibly D2-Ala260. Astashkin et al. (1995) assigned the second nitrogen to the side chain of D2-His214, based on the sequence homology between PSII and the bacterial reaction centers. Tang et al. (1995), however, excluded all histidines as a possible source of any nitrogen coupling, based on their conclusive isotope-labeling experiment. This result provides important supporting evidence to our conclusion that because of the different conformations of Q_A^- in PSII and in bacterial reaction centers, there must also exist different protein conformations at the Q_A site to accommodate the different isoprenyl-head conformations of Q_A^-.

NOTE ADDED IN PROOF

In a report which has just now appeared (Kurreck et al., 1995) on the reconstitution of exogenous PQ-9 and UQ-9 to PSII membrane fragments, inside-out vesicles, and core complexes, it was found that UQ-9 is unable to restore electron transport and O_2 evolution at a concentration for which PQ-9 gives maximum reconstitution of activity. These results further support the picture that there is a functional difference between type I and type II quinones evident in their specialized role in different electron transport proteins. The molecular basis for this functional selectivity, we claim, stems largely from the conformational difference determined by the substituent at the C6 position of the quinone ring.

ACKNOWLEDGMENT

We thank Drs. Bruce A. Diner and Xiao-Song Tang for their critical evaluation of the manuscript and for their preliminary data, and Dr. Gary Olson (Hoffmann-LaRoche Labs) for a sample of PQ-9.

REFERENCES

Astashkin, A. V., Kawamori, A., Kodera, Y., Kuroiwa, S., & Akabori, K. (1995) *J. Chem. Phys. 102*, 5583−5588.

Berthold, D. A., Babcock, G. T., & Yocum, C. F. (1981) *FEBS Lett. 134*, 231−234.

Burghaus, O., Plato, M., Rohrer, M., Mobius, K., MacMillan, F., & Lubitz, W. (1993) *J. Phys. Chem. 97*, 7639−7647.

Das, M. R., Connor, H. D., Leniart, D. S., & Freed, J. H. (1970) *J. Am. Chem. Soc. 92*, 2258−2268.

Deisenhofer, J., Epp, O., Miki, K., Huber, R., & Michel, H. (1985) *Nature 318*, 618−624.

Diner, B. A., & Petrouleas, V. (1990) *Biochim. Biophys. Acta 1015*, 141−149.

Diner, B. A., de Vitry, C., & Popot, J. L. (1988) *Biochim. Biophys. Acta 934*, 47−54.

Diner, B. A., Petrouleas, V., & Wendoloski, J. J. (1991) *Physiol. Plant 81*, 423−436.

Ermler, U., Fritzsch, G., Buchanan, S. K., & Michel, H. (1994) *Structure 2*, 925−936.

Feher, G., Isaacson, R. A., Okamura, M. Y., & Lubitz, W. (1985) *Antennas and Reaction Centers of Photosynthetic Bacteria. Structure, Interaction, and Dynamics*, pp 174−189. Springer, New York.

Ford, R. C., & Evans, M. C. W. (1983) *FEBS Lett. 160*, 159−164.

Ghanotakis, D. F., & Yocum, C. F. (1986) *FEBS Lett. 197*, 244−248.

Ghanotakis, D. F., Demetriou, D. M., & Yocum, C. F. (1987) *Biochim. Biophys. Acta 891*, 15−21.

Gunner, M. R. (1991) *Curr. Top. Bioenerg. 16*, 319−367.

Hales, B. J. (1975) *J. Am. Chem. Soc. 97*, 5993−5997.

Heller, C., & McConnell, H. M. (1960) *J. Chem. Phys. 32*, 1535−1539.

Hyde, J. S., Rist, G. H., & Eriksson, L. E. G. (1968) *J. Phys. Chem. 72*, 4269−4276.

Kevan, L., & Kispert, L. D. (1976) *Electron Spin Double Resonance Spectroscopy*, pp 199−202, John Wiley & Sons, Inc., New York.

Klimov, V. V., Dolan, E., Shaw, E. R., & Ke, B. (1980) *Proc. Natl. Acad. Sci. U.S.A. 77*, 7227−7231.

Krogmann, D. W., Olivero, E., & Duane, W. (1962) *J. Biol. Chem. 237*, 3292−3295.
Kurreck, H., Bock, M., Bretz, N., Elsner, M., Kraus, H., Lubitz, W., Muller, F., Geissler, J., & Kroneck, P. M. H. (1984) *J. Am. Chem. Soc. 106*, 737−746.
Kurreck, H., Kirste, B., & Lubitz, W. (1988) Electron Nuclear Double Resonance Spectroscopy of Radicals in Solution, VCH Publishers, Inc., New York.
Kurreck, J., Seeliger, A. G., Reifarth, F., Karge, M., & Renger, G. (1995) *Biochemistry 34*, 15721−15731.
Lykos, P. G. (1960) *J. Chem. Phys. 32*, 625−626.
MacMillan, F., Lendzian, F., Renger, G., & Lubitz, W. (1995) *Biochemistry 34*, 8144−8156.
Mattoo, A. K., Marder, J. B., & Edelman, M. (1989) *Cell 56*, 241−246.
McConnell, H., & Chesnut, D. (1958) *J. Chem. Phys. 28*, 107−117.
McLachlan, A. D. (1958) *Mol. Phys. 1*, 233−240.
Michel, H., & Deisenhofer, J. (1988) *Biochemistry 27*, 1−7.
O'Malley, P. J., & Babcock, G. T. (1984) *J. Chem. Phys. 80*, 3912−3913.
O'Malley, P. J., & Babcock, G. T. (1986) *J. Am. Chem. Soc. 108*, 3995−4001.
Okamura, M. Y., Isaacson, R. A., & Feher, G. (1975) *Proc. Nat. Acad. Sci. U.S.A. 1975*, 3491−3495.
Pederson, J. A. (1978) *Phytochemistry 17*, 775−778.
Pedersen, J. A. (1985) *CRC Handbook of EPR Spectra from Quinones and Quinols*, CRC Press, Inc., Boca Raton, FL.
Petrouleas, V., & Diner, B. A. (1990) *Biochim. Biophys. Acta 1015*, 131−140.
Sanakis, Y., Petrouleas, V., & Diner, B. A. (1994) *Biochemistry 33*, 9922−9928.
Sullivan, P. D., Bolton, J. R., & Geiger, J. W. E. (1970) *J. Am. Chem. Soc. 92*, 4176−4180.
Tang, X.-S., Peloquin, J. M., Lorigan, G. A., Britt, R. D., & Diner, B. A. (1995) Proceedings of the Xth International Congress on Photosynthesis Kluwer Academic Publishing, Dordrecht.
Trebst, A., Eck, H., & Wagner, S. (1963) *Photosynthetic Mechanisms of Green Plants*, pp 174−194, National Academy of Science, Washington, D. C.
Warncke, K., Gunner, M. R., Braun, B. S., Gu, L. Q., Yu, C. A., Bruce, J. M., & Dutton, P. L. (1994) *Biochemistry 33*, 7830−7841.
Xu, C., Taoka, S., Crofts, A. R., & Govindjee (1991) *Biochim. Biophys. Acta 1098*, 32−40.
Zheng, M., Petrouleas, V., & Dismukes, G. C. (1995) *Proceedings of the Xth International Congress on Photosynthesis* (Mathis, P., Ed.) Vol. 1, pp 763−766, Kluwer Academic Publishing, Dordrecht.

BI9522209